The Roles of Cohesive Strength and Toughness for Crack Growth in Visco-elastic and Creeping Materials

H. Wang[†], W. Lu[†], J. R. Barber[†] and M. D. Thouless[†,‡]
[†]*Department of Mechanical Engineering*
[‡]*Department of Materials Science & Engineering*
University of Michigan, Ann Arbor, MI 48109, USA

Abstract

A cohesive-zone analysis for crack propagation in a linear visco-elastic / creeping material is presented. The concept of a viscous fracture length is defined; this serves an analogous role to the elastic fracture length in determining the conditions under which fracture is controlled by the continuum crack-tip stress field. It is shown that there are two regimes for viscous crack growth. The first regime occurs in the limit of small viscous fracture lengths, when the crack-tip stress field has a region exhibiting the inverse square-root dependence expected from classical linear fracture mechanics. In this regime, the crack velocity is proportional to the fourth power of the stress-intensity factor. This is consistent with an existing analytical model developed for crack growth in linear polymers. The second regime occurs for large viscous fracture lengths, where classical fracture mechanics is not appropriate. In this regime, the crack velocity has a weaker dependence on the applied load, and can be modelled accurately by the solution to the problem of a viscous beam on an elastic foundation. At higher crack velocities, when the viscous fracture length exceeds the elastic fracture length, the expected transition to elastic fracture occurs.

April 13, 2016

1 Introduction

Modelling crack growth requires an understanding of which parameters control fracture. For example, linear-elastic fracture mechanics (LEFM) is a continuum model in which crack growth is controlled by an energy criterion; the fracture load depends only on the modulus, E, the toughness, Γ, and a dimension describing the physical size of the geometry, h (in addition to a non-dimensional description of the geometry). Generally speaking, this approach works when there is any region near the crack tip where the stresses can be described reasonably well by the continuum singular field. However, more generally, analysis of fracture requires the introduction of an additional parameter. This additional parameter can often be expressed in terms of a length associated with the fracture process. Sometimes, this length may enter the problem directly as a length over which the continuum approach breaks down, or as a critical crack-tip displacement for crack propagation. In cohesive-zone models of fracture, it enters in a dimensional fashion through a cohesive strength $\hat{\sigma}$, giving an elastic fracture length defined by $E\Gamma/\hat{\sigma}^2$, which has a unit of length.

The original motivation for this study was to determine the fracture parameters that control crack growth in a creeping solid. We addressed this by conducting a cohesive-zone analysis with a linear visco-elastic material. This analysis shows that, in contrast to when fracture is controlled by elasticity, there are no conditions under which crack growth can be modelled in a viscous or creeping material without introducing a fracture length of some description. This is true even in regimes where the crack-tip stresses exhibit a region that can be described by the continuum singular field. This conclusion is consistent with the observations of Rice [1], and with the comments of McCartney [2, 3] in response to the work of Christensen [4, 5, 6].

Time-dependent crack growth has historically been studied in two distinct areas of research: creep rupture of metals and ceramics, and fracture of polymers. Very different frameworks have been developed in each of these two areas to describe what is essentially the same problem of time-dependent crack growth. The different perspectives provided by the frameworks have resulted in what might appear to be contradictory conclusions about whether time-dependence is a desirable attribute from a fracture perspective or not. The creep-rupture literature tends to describe the problem in terms of how the time-dependent properties of a material result in sub-critical cracking at low driving forces (an apparent weakening). Conversely, the polymers literature often tends to describe the problem in terms of how the time-dependent properties of a material result in an increased rate of energy dissipation (an apparent toughening). This is, of course, merely a manifestation of the classic question of whether one is more interested in the toughness or the strength of a material system.

Crack-growth models for creeping materials are often formulated in terms of the nucleation and growth of damage in the form of cavities ahead of a crack tip [7, 8, 9]. If it is assumed that the damage is embedded within a crack-tip stress field appropriate for a creeping solid, its growth can be linked to the deformation of the surrounding material [10, 11, 12, 13]. In particular, crack advance occurs when the crack-tip region has deformed sufficiently to accommodate a critical level of damage, which may, or may not, be time-dependent. The associated analyses always require the introduction of a characteristic length beyond any continuum description of the geometry, to ensure dimensional consistency. For example, in the model of Cocks and Ashby [10], this length scale is the distance over which the damage is assumed to grow under the influence of the crack-tip stress field.

The results of models for the crack velocity in creeping materials depend on the underlying assumptions about how the damage interacts with the stress field, and how the stresses evolve at the crack tip. However, the different models share a common aspect in that the crack velocity depends on the crack-tip loading parameter for creep, C^*, which is the time-dependent analogue of the J-integral [14, 15]. The effect of creep / viscosity is to cause sub-critical crack growth until the cracks are long enough for the elastic-fracture criterion to be met, when catastrophic failure can occur. The implication of this perspective is that viscosity weakens a material, since it provides a mechanism to accommodate the growth of damage to a critical value at relatively low loads.

The mechanics of time-dependent fracture of polymers is essentially identical to that of creep rupture. However, much of the literature often focuses on the concept of a rate-dependent toughness [16, 17, 18], rather than on how the crack velocity varies with loading parameter. The viscous energy dissipated at the crack tip is seen as contributing to the toughness, and the size of the crack-tip viscous zone depends on the crack velocity [19]. The implication of this perspective is that viscosity toughens a material, since it provides a mechanism to dissipate additional energy at the crack tip.

An alternative approach used in the polymers literature introduces the concept of finite tractions behind the crack tip, following the work of Dugdale [20] and Barenblatt [21] for elastic materials. These models, such as those by Knauss[22] and Schapery [23, 24, 25], that include the interaction between a fracture-process zone and the continuum properties of the material are intellectually related to the damage-models for creep discussed earlier (although the details of the physics, and

the definition of a crack tip may differ). As a result, these models have similar forms of prediction to the creep models, in that the crack velocity increases to some power of a crack-tip loading parameter.

Cohesive-zone models of fracture represent one way to generalize these concepts into a unified framework. As discussed in the first paragraph, they automatically provide a suitable length scale to describe creep crack growth through the ratio of the toughness to the cohesive strength. Numerical analyses of time-dependent fracture using cohesive-zone elements have been developed for time-dependent [26] and time-independent [27] cohesive-zone models. In this work, we explore crack growth using a time-independent cohesive-zone model embedded in a visco-elastic material. This is essentially identical to the assumptions made in the analysis by Rahulkumar *et al.* [27] in their analysis of the peel test. These authors presented their results from the polymers perspective in which the toughness is enhanced by viscous dissipation. However, since we approached the problem from a creep-rupture perspective, our results give a different insight. (However, they are consistent with this earlier work, and can be viewed from that perspective.) Furthermore, by using the simple geometry of a moment-loaded double-cantilever beam, we have avoided a general complication that the cohesive strength can also affect the conditions for the propagation of an elastic crack. This permitted a clean relationship between the crack-growth rate and the cohesive parameters to be developed.

2 Beam Analysis

An analytical approximation for a cohesive-zone model with a linear traction-separation law of a double-cantilever beam (DCB) subjected to an applied moment of M_∞ (per unit width) can be obtained from the solution for a beam (of unit width) on an elastic foundation (Fig. 1). Owing to symmetry, and the resultant pure mode-I conditions, only one arm is considered. It is assumed that the springs are linear elastic with a spring constant k, so that they exert tractions along the beam of

$$T_n = -kv \ , \tag{1}$$

where v is the displacement of the beam. Failure of the spring occurs when its extension reaches a critical value, so that in terms of the usual parameters for a cohesive zone, the spring constant can be expressed as

$$k = \hat{\sigma}^2/\Gamma \ , \tag{2}$$

where $\hat{\sigma}$ is the cohesive strength, Γ is the toughness (recognizing that there are two halves to the DCB geometry).

2.1 Elastic analysis

If the beams are elastic, the problem and solution are well-known. The governing equation is

$$\frac{Eh^3}{12}\frac{d^4v}{dz^4} + \frac{\hat{\sigma}^2}{\Gamma}v = 0 \ . \tag{3}$$

For which a solution is given by Barber [28] as

$$\tilde{v} = \frac{2\beta_o^2 M_\infty \Gamma}{\hat{\sigma}^2 h^3} \exp^{-\beta_o \tilde{z}} \left(\cos \beta_o \tilde{z} - \sin \beta_o \tilde{z}\right) \ . \tag{4}$$

In this equation, $\tilde{v} = v/h$, $\tilde{z} = z/h$, and

$$\beta_o = \left(\frac{3kh}{E}\right)^{1/4} = \sqrt[4]{3}\tilde{\zeta}^{-1/4},$$

where $\zeta = E\Gamma/\hat{\sigma}^2$ is the elastic fracture length (for plane stress), and $\tilde{\zeta} = \zeta/h$ is the corresponding elastic fracture-length scale [29].

The stresses ahead of the crack are given by $\sigma(\tilde{z}) = -T_n(\tilde{z})$. Therefore, using Eqn. 1,

$$\frac{\sigma(\tilde{z})}{\hat{\sigma}} = \frac{kh\tilde{v}(\tilde{z})}{\hat{\sigma}} = \frac{\hat{\sigma}h}{\Gamma}\tilde{v}(\tilde{z})\,. \tag{5}$$

The condition for crack propagation can be found by equating the crack-tip stress, $\sigma(0)$ to $\hat{\sigma}$, and substituting the resulting value of $\tilde{v}(0) = \Gamma/\hat{\sigma}h$ into Eqn. 4:

$$\frac{M_\infty}{\Gamma h} = \frac{1}{\sqrt{12}}\left(\frac{Eh}{\Gamma}\right)^{1/2}\,. \tag{6}$$

This is the well-known result that the fracture condition for a DCB loaded by a pure moment depends only on the toughness, and is independent of the interfacial cohesive law. (In contrast to the case where the DCB is loaded by a point load [30].)

2.2 Viscous analysis

Using the correspondence principle, this analysis can be repeated for a linear-viscous beam. The deformation is related to the local bending moment, $M(z)$ by

$$\frac{\partial^3 v}{\partial z^2 \partial t} = -\frac{12M(z)}{\eta h^3}\,, \tag{7}$$

where η is the uniaxial viscosity, and h is the thickness of the beam. The moment is related to the tractions by

$$\frac{d^2M(z)}{dz^2} = -T_n(z) = kv(z) \tag{8}$$

If the crack is propagating at a constant velocity of $\dot{a}$, so that there is steady-state, a new non-dimensional co-ordinate can be defined as $\tilde{z} = (z - \dot{a}t)/h$. Using the non-dimensional displacement, $\tilde{v} = v/h$, Eqns. 7 and 8 can be combined to obtain the steady-state governing equation for a linear-viscous DCB:

$$\frac{d^5\tilde{v}(\tilde{z})}{d\tilde{z}^5} - \frac{12kh^2}{\eta\dot{a}}\tilde{v} = 0 \; . \tag{9}$$

The solution to this equation is of the form

$$\tilde{v}(\tilde{z}) = A \exp^{b\tilde{z}} \; , \tag{10}$$

where

$$b = [\pm\cos(\pi/5) \pm i\sin(\pi/5)]\,\lambda_o, \; b = \lambda_o \; ,$$

and

$$\lambda_o = \left(\frac{12kh^2}{\eta\dot{a}}\right)^{1/5} = \left(\frac{12\hat{\sigma}^2h^2}{\eta\Gamma\dot{a}}\right)^{1/5} \; .$$

However, only the two roots with a negative real component can contribute to the physical solution, which can be written as

$$\tilde{v}(\tilde{z}) = \exp^{-\lambda_o\tilde{z}\cos(\pi/5)} \left\{B_1\cos\left[\lambda_o\tilde{z}\sin(\pi/5)\right] + B_2\sin\left[\lambda_o\tilde{z}\sin(\pi/5)\right]\right\} \; . \tag{11}$$

The two boundary conditions for this problem are (i) the moment at the crack tip is always equal to the applied moment, so that $M(0) = -M_\infty$, and (ii) the shear force at the crack tip is 0. Therefore,

$$\left.\frac{d^3\tilde{v}}{d\tilde{z}^3}\right|_{\tilde{z}=0} = \frac{12M_\infty}{\eta h\dot{a}}$$
$$\left.\frac{d^4\tilde{v}}{d\tilde{z}^4}\right|_{\tilde{z}=0} = 0 \; . \tag{12}$$

With these boundary conditions, the solution to the steady-state crack-propagation problem is

$$\tilde{v}(\tilde{z}) = \frac{M_\infty}{\lambda_o^3 \eta h \dot{a}} \exp^{-\lambda_o \tilde{z} \cos(\pi/5)} \left\{ -12 \cos\left[\lambda_o \tilde{z} \sin(\pi/5)\right] + 16.5 \sin\left[\lambda_o \tilde{z} \sin(\pi/5)\right] \right\} \ . \quad (13)$$

As described above for the elastic case, the stresses ahead of the crack can be found from the traction distribution, and are given by

$$\frac{\sigma(\tilde{z})}{\hat{\sigma}} = \frac{kh\tilde{v}(\tilde{z})}{\hat{\sigma}} = \frac{\hat{\sigma}h}{\Gamma}\tilde{v}(\tilde{z}) \ . \quad (14)$$

The steady-state crack velocity can be found by noting that $\sigma(0)/\hat{\sigma} = 1$ at the crack tip, and by substituting the resulting value of $\tilde{v}(0) = \Gamma/\hat{\sigma}h$ into Eqn. 13:

$$\frac{\dot{a}\eta\Gamma}{\hat{\sigma}^2 h^2} = 12 \left(\frac{M_\infty}{\hat{\sigma} h^2} \right)^{2.5} \ . \quad (15)$$

The term on the left-hand side is defined here as the viscous fracture-length scale, $\tilde{\zeta_v} = \zeta_v/h$. A dimensional argument can be used to show that this is the viscous analogue of the elastic fracture-length scale, $\tilde{\zeta}$, defined earlier.[1]

3 Cohesive-zone analysis

Numerical simulations were conducted using the commercial finite-element package ABAQUS, with the cohesive-zone elements defined through a user-defined subroutine [31]. This cohesive-zone model is a mixed-mode formulation; however, the symmetry conditions of the DCB geometry ensured that this particular study was pure mode-I. The traction-separation law was chosen to be rate-independent, and of the

[1] A comparison between the elastic and viscous fracture lengths suggests that a definition of a plane-stress visco-elastic fracture length would be given by $\Gamma E(1 - \exp^{-\dot{a}\eta/Eh})/\hat{\sigma}^2 h$ for a Maxwell material.

form given by Eqn. 1. (A steep linear decay occurred after the cohesive strength had been reached; the work corresponding to this portion was 0.5 % of the work done during the rising portion of the curve.) The cohesive zone was given a finite thickness, d, corresponding to $d/h = 6.7 \times 10^{-4}$.

The constitutive properties of the arms were defined through the ABAQUS subroutine CREEP as

$$\dot{\epsilon}_{ij} = \frac{(1+\nu)\dot{\sigma}_{ij}}{E} - \frac{\nu}{E}\dot{\sigma}_{kk}\delta_{ij} + \frac{3\sigma'_{ij}}{2\eta} \ , \tag{16}$$

(using standard tensor notation), where η is the uniaxial viscosity, and σ'_{ij} is the deviatoric stress. So, a Maxwell type of material was studied, representing creep, rather than a standard-linear solid with a non-zero fully-relaxed modulus, representing a polymer. In the numerical calculations that follow, ν was set to 0.49999.

The geometry for the finite-element calculations is shown in Fig. 2. The loading couples were applied as a linear distribution of tractions to one end of each beam. The other end of each beam was clamped far ahead of the crack. The calculations were implicit, with the elements being first-order, coupled temperature-displacement, plane-stress elements, with reduced integration points (CPS4RT). To ensure accurate numerical results, the size, l_o, of the smallest element at the tip of the crack needs to be much smaller than the elastic fracture length [29]. In the present case, l_o was limited to be no larger than $10^{-4}E\Gamma/\hat{\sigma}^2$. At the lowest crack velocities, this resulted in a mesh size that could be as high as ten times the viscous fracture length. However, a mesh-sensitivity analysis showed that, even in this range, the results were mesh-insensitive within the limits of the error bars shown in the figures.

The visco-elastic calculations were done by applying a constant moment. There was an incubation period before the crack started growing. After a very short transition, the crack reached a steady-state velocity which was measured. The time increment for the calculations, Δt, was set to satisfy the condition $\dot{a}\Delta t/l_o < 50$. Within this limit there was no significant sensitivity of the results to the time increment.

4 Results

4.1 Viscous crack velocity

A dimensional analysis for the problem of a crack growing at the interface between two linear creeping beams shows that the steady-state crack velocity must be of the form

$$\frac{\dot{a}\eta}{\Gamma} = f\left(\frac{Eh}{\Gamma}, \frac{\Gamma}{\hat{\sigma}h}, \frac{M_\infty}{\Gamma h}\right) . \tag{17}$$

This function is plotted in Fig. 3, using results obtained from the cohesive-zone analysis. The asymptotic limit of rapid crack growth corresponding to elastic fracture, can be seen in this figure at the value of applied moment given by Eqn. 6. At lower levels of the applied moment, there is a viscous dominated regime, in which the first term on the right-hand side of Eqn. 17 can be neglected. Dimensional considerations show that this viscous regime is expected to occur when $\dot{a}\eta/Eh << 1$, corresponding to the viscous fracture length being much smaller than the elastic fracture length.

Figure 3 shows that there is a power-law relationship between the crack velocity and applied moment in the viscous regime. However, the power law depends on $\Gamma/\hat{\sigma}h$, and only matches the value of 2.5 given by the analytical solution of Eqn. 15 for larger values of that parameter. This issue was investigated further by a detailed

non-dimensional study of cohesive-zone results for the crack velocity in the viscous regime. It was found empirically that, when non-dimensionalized as

$$\frac{\dot{a}\eta\Gamma}{\hat{\sigma}^2 h^2} = f\left(\frac{M_\infty}{\hat{\sigma}h^2}\right) , \tag{18}$$

the crack velocity can be expressed as a function of a single non-dimensional group, instead of the two non-dimensional groups predicted by Eqn. 17.

The master curve that arises from the normalization described above is shown in Fig. 4. It will be seen that the analytical result from beam theory (Eqn. 15) is valid when the viscous fracture-length scale is greater than unity. For smaller viscous fracture-length scales, an empirical fit to the data suggests that

$$\frac{\dot{a}\eta\Gamma}{\hat{\sigma}^2 h^2} \approx 70\left(\frac{M_\infty}{\hat{\sigma}h^2}\right)^4 . \tag{19}$$

The fact that there are two regimes of behavior, depending on the fracture-length scale, is very reminiscent of what is seen with elastic fracture. In elastic fracture, small fracture-length scales correspond to a regime of toughness-controlled fracture, with the stress fields exhibiting a region over which the stresses follow an inverse square-root dependence on the distance ahead of a crack tip. Conversely, large fracture-length scales correspond to a regime of strength-controlled fracture, and the crack-tip stress fields have no region over which there is an inverse square-root dependence. This generalization is complicated in the special case of a moment-loaded double-cantilever beam, because the elastic fracture strength depends only on toughness; the cohesive strength does not affect the conditions for fracture in a DCB loaded in this fashion. However, as will be shown below, the general effect of fracture-length scales on crack-tip stress fields can be demonstrated with this geometry.

4.2 Crack-tip stresses

For any specified form of cohesive law, the normal stresses ahead of a crack in an elastic double-cantilever-beam geometry can be expressed as[2]

$$\frac{\sigma}{\hat{\sigma}} = f\left(\frac{z}{h}, \frac{M_\infty}{\hat{\sigma}h^2}, \frac{E\Gamma}{\hat{\sigma}^2 h}\right) \ . \tag{20}$$

In the special case of a linear traction-separation law for the cohesive zone, this reduces to [32]

$$\sigma/\hat{\sigma} = f\left(\tilde{z}, \tilde{\zeta}\right) \ . \tag{21}$$

In the limit of $\tilde{\zeta}$ going to zero, the linear-elastic solution predicts that the stresses scale with $\tilde{z}^{-0.5}$ close to the crack tip. As $\tilde{\zeta}$ increases, the region over which the stresses follow an inverse-square-root relationship moves away from the crack tip and decreases in size. Eventually, when $\tilde{\zeta}$ is greater than about 0.4, there is no region over which the stresses show any inverse-square-root dependency [33, 32]. This can be seen in the results of Fig. 5, where the stress distributions from cohesive-zone analyses for relatively small and large values of $\tilde{\zeta}$ are compared to the LEFM stress field. Superimposed on these plots are the corresponding stress distributions of Eqn. 5. It will be seen from these plots that elastic-foundation analyses provide very accurate results for stress distributions if the fracture-length scale is large. However, they do not capture the singular fields appropriate for small fracture-length scales.

The normal stresses ahead of a crack in a viscous double-cantilever-beam geometry can be expressed in a similar form to Eqn. 21; they depend only on $\tilde{z}$ and $\tilde{\zeta}_v$. These stresses are shown in Fig. 6, and it can be seen that they have an analogous form to the

[2] A dimensional analysis suggests there should be four groups, but the use of the fracture-length scale allows two of the groups to be combined.

stresses ahead of a crack in an elastic geometry. The viscous-beam solution provides a good description of the stresses ahead of a crack when the viscous fracture-length scale is large, but does not do so for small values. The inverse square-root singular field that is expected for a linear material when $\tilde{\zeta}_v$ is small, is not captured by the beam solution, but it is captured by the cohesive-zone model. Conversely, when $\tilde{\zeta}_v$ is large, beam theory does describe the stress field reasonably accurately, agreeing with the cohesive-zone model.

5 Discussion

A summary of the three different regimes of visco-elastic creep-crack growth can be seen in Fig. 7. In this particular geometry, the elastic fracture condition is given by the LEFM solution of Eqn. 6, irrespective of the fracture-length scale. Therefore, if

$$\frac{M_\infty}{\hat{\sigma}h^2} > \frac{1}{\sqrt{12}}\left(\frac{E\Gamma}{\hat{\sigma}^2 h}\right)^{1/2}, \tag{22}$$

there is no equilibrium solution, and the crack must propagate dynamically. As the applied bending moment approaches this limiting value, the crack velocity increases dramatically. If $M_\infty/\hat{\sigma}h^2$ is significantly below this value, then the crack velocity is given by either Eqn. 15 or Eqn. 19:

$$\frac{\dot{a}\eta\Gamma}{\hat{\sigma}^2h^2} = 12\left(\frac{M_\infty}{\hat{\sigma}h^2}\right)^{2.5}, \text{ if } \frac{\dot{a}\eta\Gamma}{\hat{\sigma}^2h^2} > 1$$
$$\frac{\dot{a}\eta\Gamma}{\hat{\sigma}^2h^2} \approx 70\left(\frac{M_\infty}{\hat{\sigma}h^2}\right)^{4}, \text{ if } \frac{\dot{a}\eta\Gamma}{\hat{\sigma}^2h^2} < 0.1\,,$$

with a transition between the two limits. Both behaviors will only be observed for relatively tough materials. For example, Fig. 7 shows that brittle materials exhibit only the second type of viscous crack growth when elastic fracture occurs at too low

a value of the applied moment.

In small-scale damage-zone models of creep-rupture in linear materials, the crack velocity is predicted to be proportional to K, the stress-intensity factor (where, $K = \sqrt{\eta C^*}$). For example, the model of Cocks and Ashby [10] gives a crack velocity of

$$\frac{\eta \dot{a}}{\Gamma} = \sqrt{\frac{2}{\pi}} \frac{K r_o^{1/2}}{\epsilon_c \Gamma} \ , \tag{23}$$

where r_o is the length of the damage zone, and ϵ_c is the critical strain for material at the crack tip. For the geometry modeled in this paper, the stress-intensity factor is given by

$$K^2 = 12 M_o^2 / h^3 \ . \tag{24}$$

Therefore, when the viscous fracture-length scale is small and the stress field has a region over which the stresses follow an inverse square-root dependence, the crack velocity should depend on K. Under these conditions, one can use Eqns. 19 and 24 to show that

$$\frac{\eta \dot{a}}{\Gamma} = 0.5 \left(\frac{K^2}{\Gamma \hat{\sigma}} \right)^2 \ . \tag{25}$$

As expected for this limit, the geometrical parameters enter the description of the problem only through the stress-intensity factor, and do not otherwise affect the crack velocity.

Although both the small-scale damage model and the cohesive-zone model with a small fracture-length scale emphasize how the geometrical parameters affect the crack velocity only through the stress-intensity factor, the dependence on K is different for the two models. One reason for this discrepancy may arise from how the characteristic length for fracture is introduced in both models. In the creep-rupture model, it is introduced as a material constant, r_o. In the cohesive-zone model, the viscous

fracture-length scale is a variable that depends on the crack velocity.

Schapery [23, 24, 25] developed an analytical model for crack growth in visco-elastic materials. This analysis assumed a crack tip with a singular stress field, and a small-scale region of non-linear and finite cohesive tractions behind it. This is analogous to a perspective in which a damage zone ahead of a crack tip is viewed as a bridging zone behind a crack tip, with the arbitrariness of such a distinction becoming obvious in a cohesive-zone model [32]. Equation 56 in Ref. [24] can be expressed in terms of the parameters used in this paper:

$$\frac{\eta \dot{a}}{\Gamma} = \frac{0.8\pi}{3} \left(\frac{K^2}{\Gamma \sigma_m I_1} \right)^2 \ . \tag{26}$$

In this equation, the quantity $\sigma_m I_1$ is identified as a second fracture parameter, with σ_m being the maximum stress in the bridging zone behind the crack tip, and I_1 being a numerical constant that relates K and σ_m to the size of the non-linear zone behind the crack tip.

If one assumes that σ_m is the analytical model can be identified with $\hat{\sigma}$ in the present linear-hardening cohesive-zone model, a comparison between Eqns. 25 and 26 shows that a value of $I_1^2 = 1.6\pi/3$ would give an exact match between the two solutions. I_1 is related to the length of the non-linear zone behind the crack tip, α, through [24]

$$\alpha = (\pi/2) \left(K/\sigma_m I_1 \right)^2 \ . \tag{27}$$

Therefore, using the value of I_1 given above, this quantity α can be equated to the viscous fracture-length scale as

$$\alpha/h \approx 1.3\sqrt{\tilde{\zeta}_v} \ . \tag{28}$$

There is no singular crack tip in a cohesive zone model, so making a rigorous connection to α is not possible. However, it is of interest to note from Fig. 6(a) that the distance from the crack tip over which the stresses can be described by an inverse-square-root field is $0.03 \leq z/h \leq 0.06$, compared to a value of $\alpha/h = 0.08$, when $\tilde{\zeta_v} = 0.0034$.

The polymers literature also presents alternative perspectives in which the crack velocity is related to an effective toughness that includes a viscous dissipation term. For example, the cohesive-zone analysis of Rahulkumar *et al.* [27] shows that the peak dissipation (and maximum effective toughness) occurs at intermediate crack velocities. At high and low velocities, the crack-tip material is loaded in the unrelaxed and relaxed elastic regimes, so there is limited viscous dissipation, and the effective toughness tends to the intrinsic toughness, Γ. A similar calculation for the viscous dissipation in the present model shows that the effective toughness increases without limit as the crack speed decreases, as would be expected for a system in which the fully-relaxed modulus is zero.

In the light of this discussion, one can appreciate how a standard-linear solid might behave if approached from the vantage point of the present paper. Two elastic fracture-length scales would be introduced: an unrelaxed fracture-length scale, $\zeta_u = E_u\Gamma/\hat{\sigma}^2 h$. where E_u is the unrelaxed modulus, and a fully-relaxed fracture-length scale, $\zeta_r = E_r\Gamma/\hat{\sigma}^2 h$. where E_r is the fully relaxed modulus. From Eqn. 6, it can be seen that there can be no crack propagation when

$$\frac{M_\infty}{\hat{\sigma}h^2} < \sqrt{\frac{\zeta_r}{12}}\,. \tag{29}$$

Above this value, the slower mode of viscous crack growth will be observed only

if $\zeta_r < 0.45$, and the faster mode of viscous crack growth will be observed only if $\zeta_u > 1.6$. A further exploration of this topic is beyond the scope of the present paper, although the general notion that there is an upper and lower bound for elastic crack growth is consistent with the results of Rahulkumar *et al.* [27].

6 Conclusions

A cohesive-zone analysis of linear visco-elastic crack growth for a double-cantilever-beam geometry shows three distinct regimes of behavior. At low velocities, corresponding to small viscous fracture lengths when the crack-tip stress field is controlled by the stress-intensity factor, the crack velocity scales with K^4. This regime has the same characteristics as an earlier analytical model for K-field dominated crack growth in polymers [23, 24]. At higher crack velocities, corresponding to higher viscous fracture lengths, the stress field can be modeled as a viscous beam on an elastic foundation. Under these conditions, there is no inverse square-root stress field, and the crack velocity grows with a much lower dependence on the applied load. At very high loads, there is a transition towards elastic fracture with a dramatic increases in the crack velocity.

The results in this study have been presented for a simple geometry that exhibits a steady state, and for which the elastic-fracture condition is independent of the fracture-length scale. This ensures that the elastic fracture condition is uniquely described by the toughness only. There will be an even richer behavior for visco-elastic crack growth in more general geometries, for which the elastic-fracture condition depends on the elastic fracture-length scale. It is further noted that a more general

visco-elastic model, with a non-zero relaxed modulus, is expected to truncate the viscous crack growth at low velocities, providing a threshold for crack growth.

The results in this paper have been presented from a perspective commonly used in creep-rupture. From this perspective, viscosity serves to make a material weak, causing sub-critical crack growth when the loads are lower than those required to cause elastic fracture. However, it is noted that the results are consistent with a common polymers perspective in which the apparent toughness increases as the crack velocity decreases, owing to the increase in viscous dissipation. Rather than making the material weak, viscosity can be seen to make the material tougher. Obviously, this dichotomy in the two perspectives is a long-standing one, and the question of whether one might prefer a tough but weak material or a strong but brittle material depends on the application. However, the numerical crack-propagation model presented here, in which the crack velocity can be related to both the applied load and the energy dissipation, serves as a nice illustration of the issue.

Finally, it is noted that the analysis presented in this paper follows an assumption commonly used in both the creep-rupture and polymer-fracture literature, of assuming that the rate-controlling time dependence arises from the bulk deformation of the material, not from the fracture phenomena. The fracture processes have been assumed to be rate-independent. Cohesive-zone models that incorporate rate dependences for both the bulk deformation and the fracture process are certainly possible, but beyond the scope of the present paper. One can however, get a sense of how the rate dependence of either the toughness or the cohesive strength might affect the crack velocity, by using the current results and making suitable assumptions about how both parameters might change with crack velocity.

Acknowledgements

This research was supported by the Consortium for Advanced Simulation of Light Water Reactors (http://www.casl.gov), an Energy Innovation Hub (http://www.energy.gov/hubs) for Modeling and Simulation of Nuclear Reactors under U.S. Department of Energy Contract No. DE-AC05-00OR22725.

References

[1] J. R. Rice. The mechanics of quasi-static crack growth. In R. E. Kelly, editor, *US. National Congress on Theoretical and Applied Mechanics*, pages 191–216. Western Periodicals Co., North Hollywood, CA, 1979.

[2] L. N. McCartney. Discussion of "A rate-dependent criterion for crack growth" by R. M. Christensen. *International Journal of Fracture*, 16:R229–R232, 1980.

[3] L. N. McCartney. Response to discussion concerning kinetic criteria for crack in viscoelastic materials. *International Journal of Fracture*, 17:R161–R168, 1981.

[4] R. M. Christensen. A rate-dependent criterion for crack growth. *International Journal of Fracture*, 15:3–21, 1979.

[5] R. M. Christensen. Response: Discussion of "A rate-dependent criterion for crack growth" by L. N. McCartney. *International Journal of Fracture*, 16:R233–R237, 1980.

[6] R. M. Christensen. Viscoelastic crack growth - a response note. *International Journal of Fracture*, 17:R169–R176, 1981.

[7] D. S. Wilkinson and V. Vitek. The propagation of cracks by cavitation: a general theory. *Acta Metallurgica*, 30:1723–1732, 1982.

[8] J. L. Bassani and V. Vitek. Propagation of cracks under creep conditions. In *Proceedings of 9th U.S. National Congress on Theoretical and Applied Mechanics*, pages 127–133, 1982.

[9] M. D. Thouless, C. H. Hsueh and A. G. Evans. A damage model of creep crack growth in polycrystals. *Acta Metallurgica*, 31:1675–1687, 1983.

[10] A. C. F. Cocks and M. F. Ashby. The growth of a dominant crack in a creeping material. *Scripta Metallurgica*, 16:109–114, 1982.

[11] C. Y. Hui and V. Banthia. The extension of cracks at high temperature by growth and coalescence of voids. *International Journal of Fracture*, 25:53–67, 1984.

[12] H. Riedel. Creep crack growth under small-scale creep conditions. *International Journal of Fracture*, 42:173–188, 1990.

[13] J. L. Bassani and D. E. Hawk. Influence of damage on crack-tip fields under small-scale-creep conditions. *International Journal of Fracture*, 42:157–172, 1990.

[14] J. D. Landes and J. A. Begley. A fracture mechanics approach to creep crack growth. In J. R. Rice and P. C. Paris, editors, *Mechanics of Materials*, volume STP 590, pages 128–148. ASTM International, 1976.

[15] C. E. Turner K. M. Nikbin, G. A. Webster. Relevance of nonlinear fracture mechanics to creep cracking. In J. L. Swedlow and M. L. Williams, editors, *Cracks and Fracture*, volume STP 601, pages 47–62. ASTM International, 1976.

[16] E. H. Andrews and A. J. Kinloch. Mechanics of adhesive failure. I. *Proceedings of the Royal Society of London*, A332:385–399, 1973.

[17] R.-J. Chang and A. N. Gent. Effect of interfacial bonding on the strength of adhesion of elastomers. I Self-adhesion. *Journal of Polymer Science*, 19:1619–1633, 1981.

[18] J. G. Williams. *Fracture Mechanics of Polymers*. Ellis Horwood, Chichester, UK, 1984.

[19] D. B. Xu and C.-Y. Hui. Interface fracture and viscoelastic deformation in finite size specimens. *Journal of Applied Physics*, 72:3305–3316, 1992.

[20] D. S. Dugdale. Yielding of steel sheets containing slitsl. *Journal of the Mechanics and Physics of Solids*, 8:100–104, 1960.

[21] G. I. Barenblatt. The mathematical theory of equilibrium cracks in brittle fracture. In *Advances in Applied Mechanics*, volume 7, pages 55–129. Academic Press, NY, USA, 1962.

[22] W. G. Knauss. Delayed failure - the Griffith problem for linearly viscoelastic materials. *International Journal of Fracture Mechanics*, 6:7–20, 1970.

[23] R. A. Schapery. A theory of crack initiation and growth in viscoelastic media: I Theoretical development. *International Journal of Fracture*, 11:141–159, 1975.

[24] R. A. Schapery. A theory of crack initiation and growth in viscoelastic media: II Approximate methods of analysis. *International Journal of Fracture*, 11:369–388, 1975.

[25] R. A. Schapery. A theory of crack initiation and growth in viscoelastic media: II Analysis of continuous growth. *International Journal of Fracture*, 11:549–562, 1975.

[26] C. M. Landis, T. Pardoen and J. Hutchinson. Crack velocity dependent toughness in rate dependent materials. *Mechanics of Materials*, 32:663–678, 2000.

[27] P. Rahulkumar, A. Jagota, S. J. Bennison and S. Saigal. Cohesive element modeling of viscoelastic fracture: application to peel testing of polymers. *International Journal of Solids and Structures*, 37:1873–1897, 2000.

[28] J. R. Barber. *Intermediate Mechanics of Materials*. Springer, Dordrecht, The Netherlands, 2011.

[29] M. D. Thouless and R. B. Sills. The effect of cohesive-law parameters on mixed-mode fracture. *Engineering Fracture Mechanics*, 109:353–368, 2013.

[30] S. Li, J. Wang and M. D. Thouless. The effects of shear on delamination of beam-like geometries. *Journal of the Mechanics and Physics of Solids*, 52:193–214, 2004.

[31] Q. D. Yang and M. D. Thouless. Mixed-mode fracture analyses of plastically-deforming adhesive joints. *International Journal of Fracture*, 110:175187, 2001.

[32] M. D. Thouless and R. B. Sills. Cohesive-length scales for damage and toughening mechanisms. *International Journal of Solids and Structures*, 55:32–43, 2015.

[33] J. P. Parmigiani and M. D. Thouless. The effects of cohesive strength and toughness on mixed-mode delamination of beam-like geometries. *Engineering Fracture Mechanics*, 74:2675–2699, 2007.

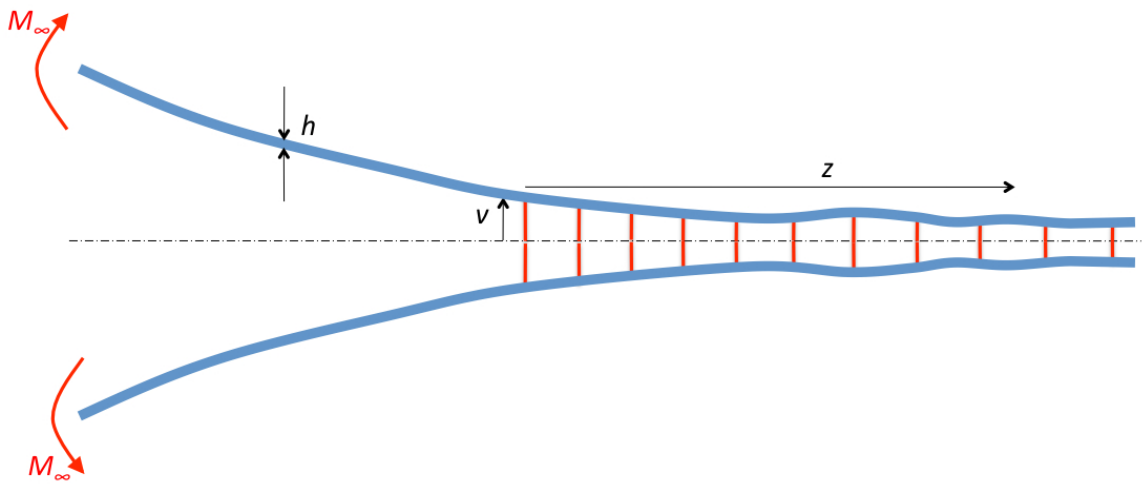

Figure 1: Geometry of a DCB with elastic springs along the interface.

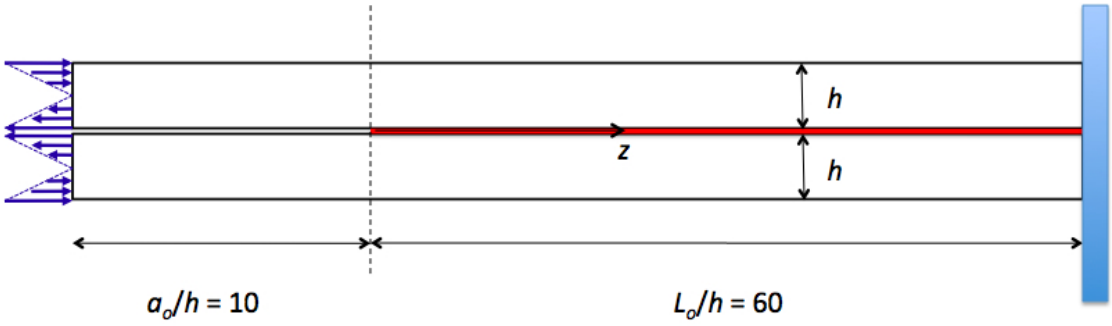

(a)

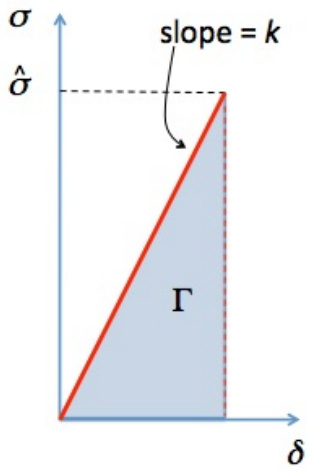

(b)

Figure 2: **(a)** Double-cantilever beam geometry, with arms of thickness h, used for the cohesive-zone analysis. The initial crack is of length $a_o/h = 10$, and is loaded by a distribution of forces that gives a pure moment M_∞. Linear-hardening cohesive elements with the traction-separation law shown in **(b)** were used along the entire bonded interface.

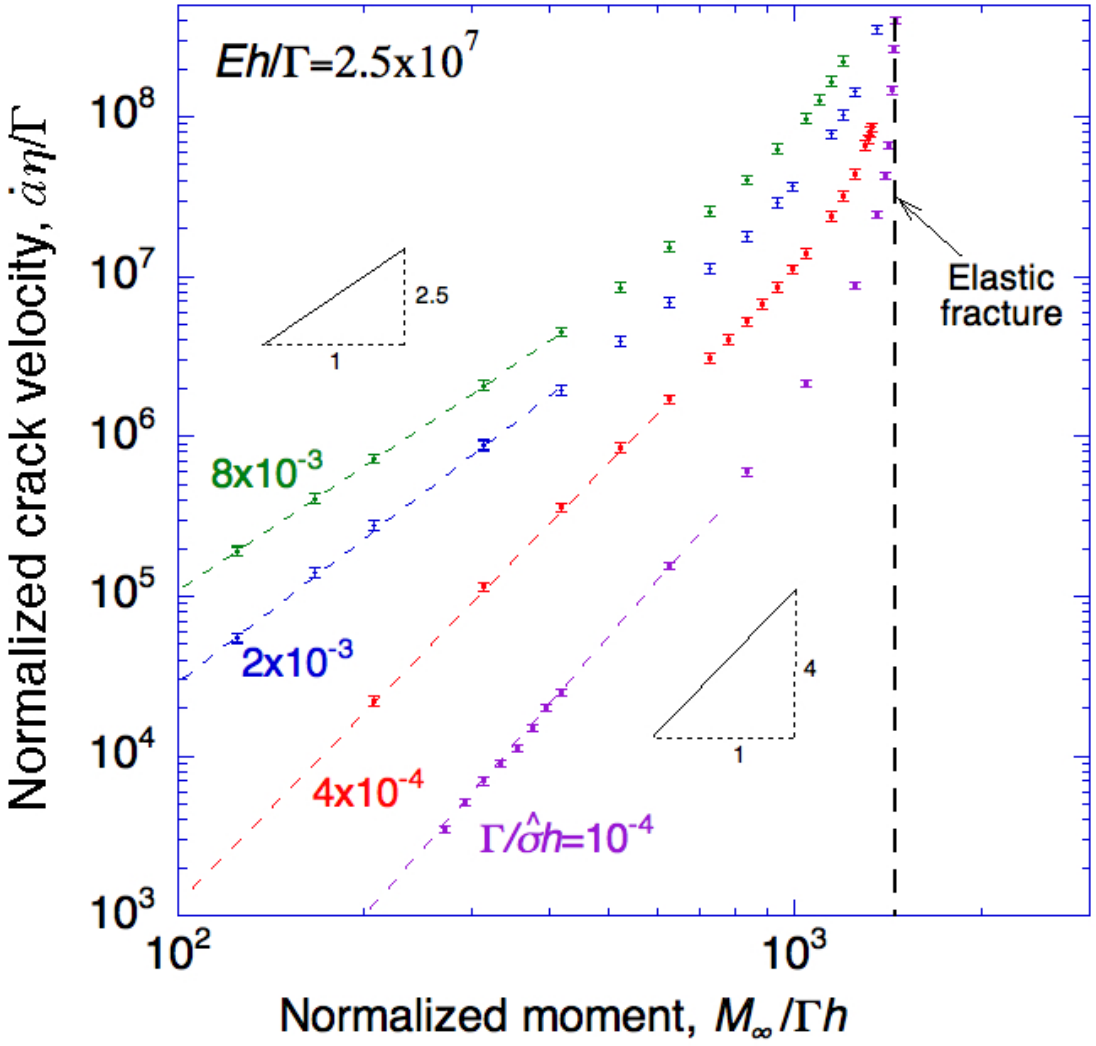

Figure 3: Non-dimensional crack velocity plotted as a function of applied moment. As the magnitude of the applied moment approaches the value for elastic fracture, the crack velocity increases without limit. At lower values of the applied moment, the crack velocity depends only on the viscous properties of the DCB arms, not on the elastic properties.

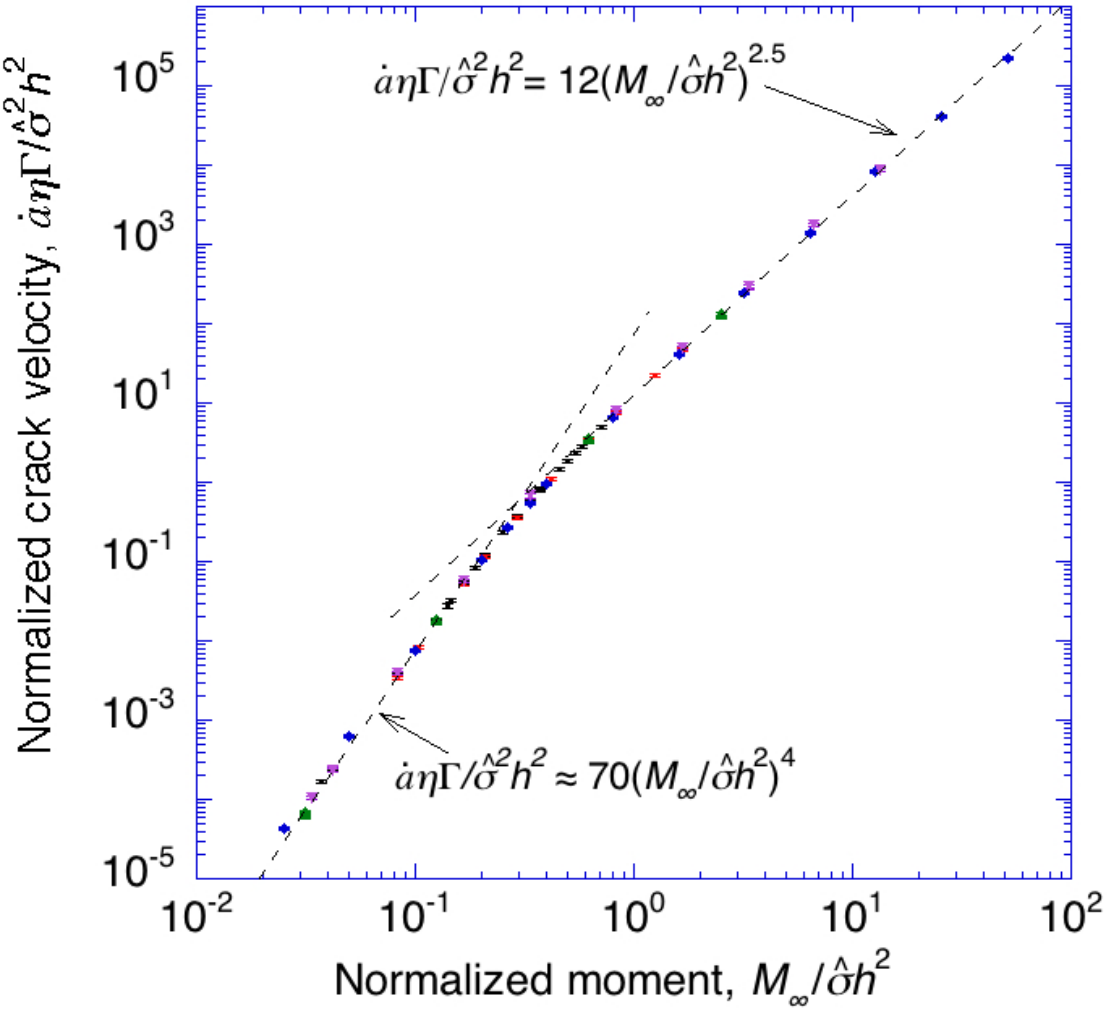

Figure 4: Non-dimensional crack velocity (viscous fracture-length scale) plotted as a function of applied moment in the viscous regime, showing two regimes of behavior. The transition between these two regimes of behavior occurs when the viscous fracture-length scale is approximately equal to one. The data plotted in this figure represent a range of different combinations of the two non-dimensional groups that are not represented on the axes of the figure. While doing the calculations, the parameters were kept in a range that ensured viscous crack growth, with Eh/Γ being between 2.5×10^7 and 5×10^{10}, and $\Gamma/\hat{\sigma}h$ being between 10^{-5} and 5×10^{-3}.

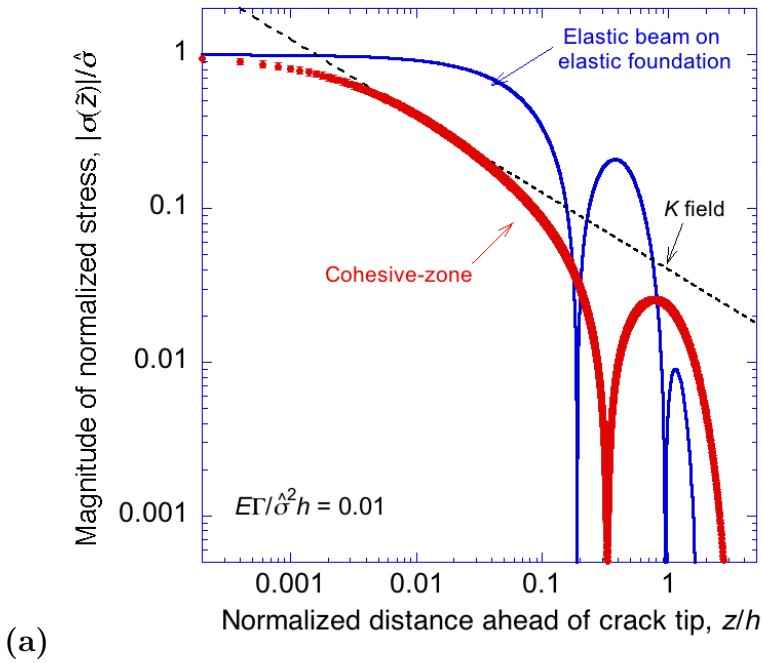

(a)

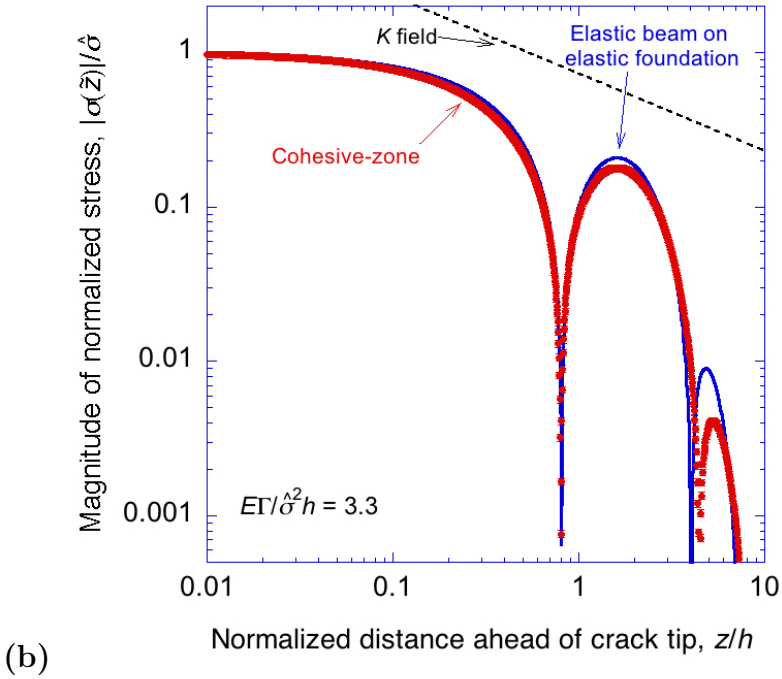

(b)

Figure 5: Comparison between the stress distributions ahead of a crack in an elastic double-cantilever beam, using the results from a cohesive-zone model and an elastic foundation model. **(a)** A relatively small elastic fracture-length scale of $\tilde{\zeta} = 0.01$, and **(b)** a relatively large elastic fracture-length scale of $\tilde{\zeta} = 3.3$. No other dimensionless groups affect the stress distributions. The oscillations correspond to alternating regions of tension and compression, as expected for a beam loaded by a pure moment with no net force normal to the crack plane.

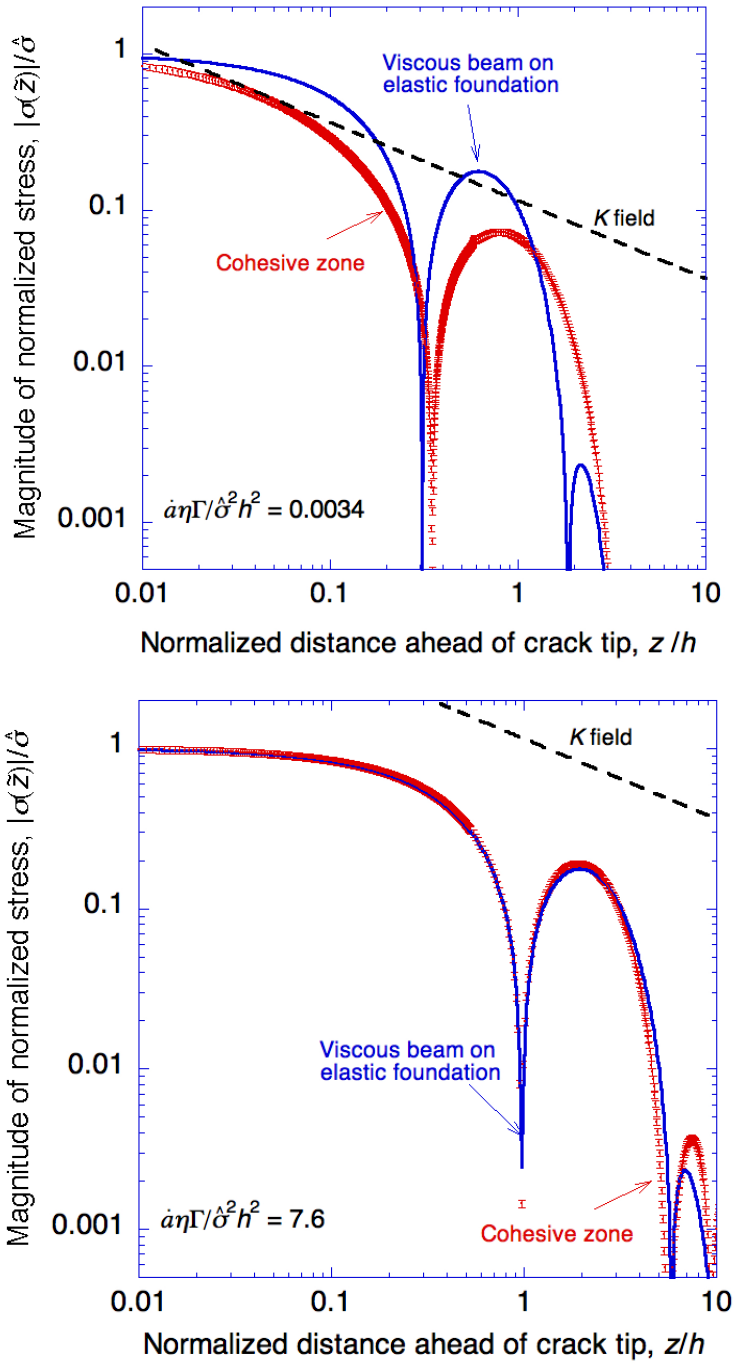

Figure 6: Comparison between the stress distributions ahead of a crack in an viscous double-cantilever beam, using the results from a cohesive-zone model and an elastic foundation model. **(a)** A relatively small viscous fracture-length scale of $\tilde{\zeta}_v = 0.0034$, and **(b)** a relatively large viscous fracture-length scale of $\tilde{\zeta}_v = 7.6$. For both of these calculations, the elastic fracture-length scale was equal to 250, which is much larger than the viscous fracture-length scales. Therefore, both sets of results are well within the viscous limit.

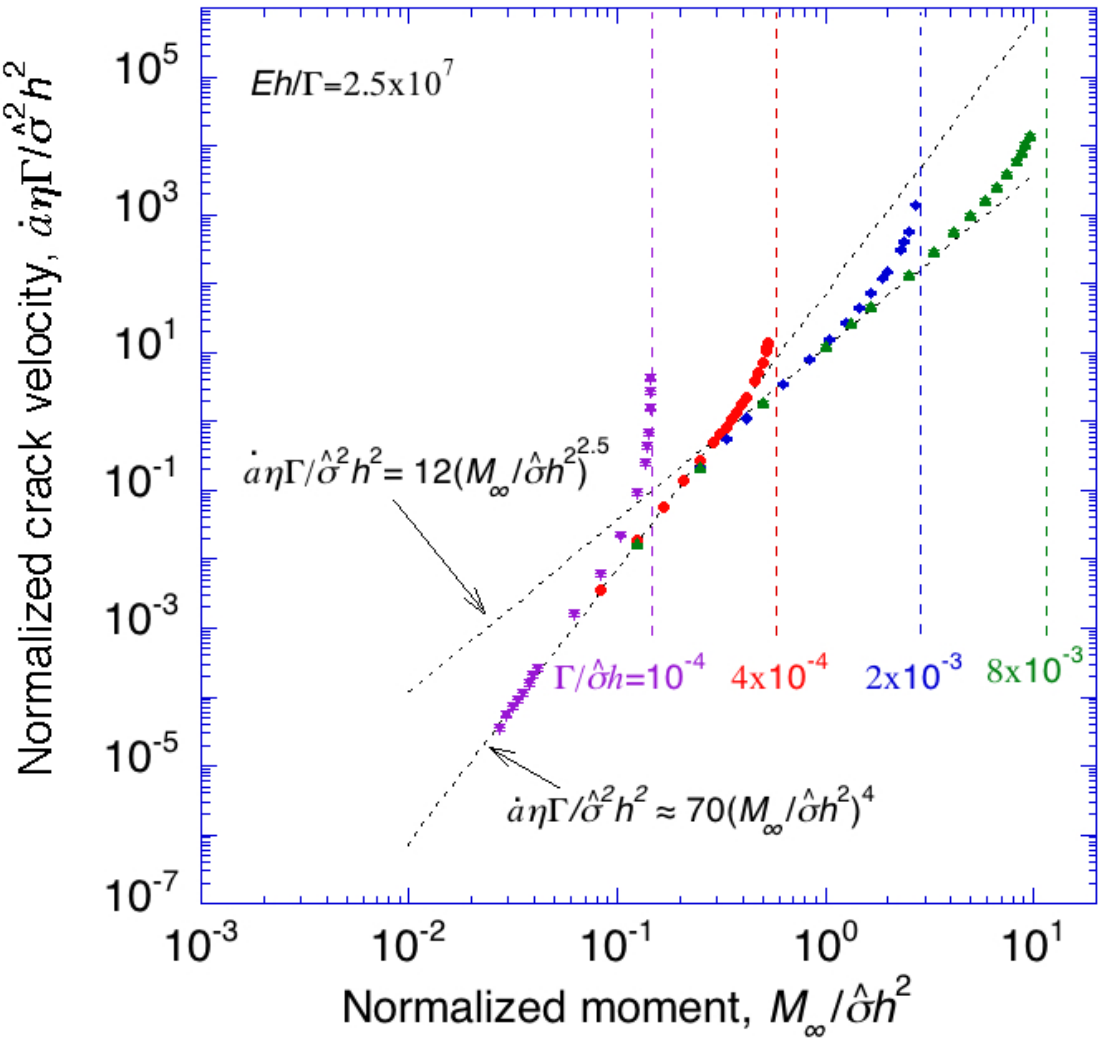

Figure 7: A summary of the three different crack-growth regimes, showing elastic fracture, crack growth at large viscous fracture lengths, and crack growth at small viscous fracture lengths. The crack velocity increases significantly as the applied moment approaches the critical moment for elastic fracture.